Reactions Catalyzed by Tetrahydrobiopterin-Free Nitric Oxide Synthase†

Kristin M. Rusche,‡ Michelle M. Spiering,§ and Michael A. Marletta*,‡,§,||

Department of Biological Chemistry, School of Medicine, Interdepartmental Program in Medicinal Chemistry, and Howard Hughes Medical Institute, The University of Michigan, Ann Arbor, Michigan 48109-1065

Received June 15, 1998; Revised Manuscript Received August 10, 1998

ABSTRACT: Murine macrophage nitric oxide synthase (NOS) was expressed in *E. coli* and purified in the presence (holoNOS) or absence (H_4B-free NOS) of (6*R*)-tetrahydro-L-biopterin (H_4B). Isolation of active enzyme required the coexpression of calmodulin. Recombinant holoNOS displayed similar spectral characteristics and activity as the enzyme isolated from murine macrophages. H_4B-free NOS exhibited a Soret band at approximately 420 nm and, by analytical gel filtration, consisted of a mixture of monomers and dimers. H_4B-free NOS catalyzed the oxidation of N^G-hydroxy-L-arginine (NHA) with either hydrogen peroxide (H_2O_2) or NADPH and O_2 as substrates. No product formation from arginine was observed under either condition. The amino acid products of NHA oxidation in both the H_2O_2 and NADPH/O_2 reactions were determined to be citrulline and N^δ-cyanoornithine (CN-orn). Nitrite and nitrate were also formed. Chemiluminescent analysis did not detect the formation of nitric oxide (•NO) in the NADPH/O_2 reaction. The initial inorganic product of the NADPH/O_2 reaction is proposed to be the nitroxyl anion (NO^-) based on the formation of a ferrous nitrosyl complex using the heme domain of soluble guanylate cyclase as a trap, and the formation of a ferrous nitrosyl complex of H_4B-free NOS during turnover of NHA and NADPH. NO^- is unstable and, under the conditions of the reaction, is oxidized to nitrite and nitrate. At 25 °C, the H_2O_2-supported reaction had a specific activity of 120 ± 14 nmol min^{-1} mg^{-1} and the NADPH-supported reaction had a specific activity of 31 ± 6 nmol min^{-1} mg^{-1} with a $K_{M,app}$ for NHA of 129 ± 9 μM. HoloNOS catalyzed the H_2O_2-supported reaction with a specific activity of 815 ± 30 nmol min^{-1} mg^{-1} and the NADPH-dependent reaction to produce •NO and citrulline at 171 ± 20 nmol min^{-1} mg^{-1} with a $K_{M,app}$ for NHA in the NADPH reaction of 36.9 ± 0.3 μM.

The formation of •NO and citrulline from arginine is catalyzed by nitric oxide synthase (NOS,[1] EC 1.14.13.39) (*1*). The reaction requires NADPH and O_2 and proceeds via the intermediate N^G-hydroxy-L-arginine (NHA) (*2*, *3*). The enzyme has three distinct isoforms: a membrane-associated, constitutive enzyme from the vascular endothelium (*4*); a soluble, constitutive enzyme from neuronal cells (*5*, *6*); and an endotoxin- and cytokine-inducible enzyme exemplified by that from murine macrophages (*7*, *8*). The constitutive enzymes are regulated by the binding of Ca^{2+} and calmodulin (*5*, *6*), whereas the inducible enzyme binds calmodulin tightly and the activity is not regulated by Ca^{2+} (*9*, *10*). The enzyme is homodimeric with an equivalent of FAD, FMN (*7*, *8*, *11*, *12*), and iron protoporphyrin IX heme (*12*−*15*) per subunit. In addition, H_4B is required for full activity of all isoforms and was shown to bind stoichiometrically (*11*, *12*, *16*).

Proposals regarding the NOS catalytic mechanism have invoked the H_4B cofactor, others, solely the P450-type heme cofactor. Support for the participation of heme in the NOS-catalyzed oxidation of NHA to citrulline and •NO has been obtained from carbon monoxide (CO) inhibition studies (*17*) and from studies on the substitution of hydrogen peroxide (H_2O_2) for NADPH and O_2 in the catalytic cycle (*18*, *19*). The mechanism proposed for the steroidogenic P450 aromatase, nucleophilic attack by an iron peroxide intermediate, has also been proposed for the NOS-catalyzed reaction with NHA (*18*). CO inhibition of the conversion of arginine to citrulline and •NO suggests the participation of heme in the N-hydroxylation of arginine to NHA (*13*). However, the inability of NOS to catalyze arginine oxidation by H_2O_2 or iodosobenzene (*18*) argues against the participation of heme in the first step of the reaction. The aromatic amino acid hydroxylases utilize H_4B in catalyzing reactions with phenylalanine, tyrosine, and tryptophan (*20*, *21*). A similar role for H_4B in the first step of the NOS reaction may be envisioned. However, no direct evidence to support this role has emerged. A recent crystal structure of the heme domain dimer of inducible NOS (*22*) reveals the H_4B cofactor bound at the edge of and perpendicular to the heme plane. Arginine was shown bound with the guanidinium group over heme

† This research was supported by NIH Grants CA50414 and CA26731 and by the Howard Hughes Medical Institute.

* To whom correspondence should be addressed.

‡ Department of Biological Chemistry, University of Michigan.

§ Interdepartmental Program in Medicinal Chemistry, University of Michigan.

|| Howard Hughes Medical Institute.

[1] Abbreviations: NOS, nitric oxide synthase; iNOS, inducible nitric oxide synthase; CaM, calmodulin; H_4B, (6*R*)-tetrahydro-L-biopterin; *q*-H_2B, quinonoid dihydrobiopterin; NHA, N^G-hydroxy-L-arginine; H_2O_2, hydrogen peroxide; CN-orn, N^δ-cyanoornithine; •NO, nitric oxide; NO^-, nitroxyl anion; sGC, soluble guanylate cyclase; β1(1−385), heme domain of sGC; DTT, dithiothreitol; HPLC, high-performance liquid chromatography; SDS−PAGE, sodium dodecyl sulfate−polyacrylamide gel electrophoresis; *o*-PA, *o*-phthalaldehyde; NDA, 2,3-naphthalenedicarboxaldehyde; P450, cytochrome P450; NO_2^-, nitrite; NO_3^-, nitrate; Hepes, 4-(2-hydroxyethyl)-1-piperazineethanesulfonic acid; CO, carbon monoxide; IPTG, isopropyl β-D-thiogalactopyranoside.

10.1021/bi9813936 CCC: $15.00
Published on Web 10/16/1998

pyrrole ring A, considerably distant from the H_4B cofactor. The crystal structure of the heme domain, therefore, does not support a role for pterin in directly hydroxylating arginine.

To investigate the function of H_4B in NOS catalysis, we have expressed murine macrophage iNOS in *E. coli* and purified the enzyme in the presence and absence of H_4B. Since bacteria do not produce H_4B, purification of NOS in the absence of added H_4B results in H_4B-free NOS. We report here on the properties and catalytic activity of H_4B-free NOS. Lack of arginine reactivity and the formation of citrulline, N^{δ}-cyanoornithine (CN-orn), and NO^- from NHA have potentially important mechanistic implications for the role of H_4B in NOS catalysis.

EXPERIMENTAL PROCEDURES

Materials and General Methods. *E. coli* JM109 competent cells, T4 DNA ligase, and IPTG were from Gibco-BRL. All restriction enzymes, alkaline phosphatase, ampicillin, chloramphenicol, and the Expand High Fidelity PCR kit were purchased from Boehringer Mannheim. QIAfilter Plasmid kit and QIAquick Gel Extraction kit were purchased from Qiagen. The subcloning plasmid pGEM-4Z was purchased from Promega. iNOS clone in pBluescript II KS was a gift from Dr. James M. Cunningham (Brigham and Women's Hospital, Boston, MA). The pCWori plasmid (ampicillin resistance, tac-tac promoter) was a gift from Dr. Michael R. Waterman (Vanderbilt University). The plasmid/gene construct pACYC:CaM2-1 (chloramphenicol resistance, tac promoter, pUC ori) was used without modification (*23*). H_4B was purchased from Dr. B. Schirks Laboratory (Jona, Switzerland) and prepared in 100 mM Hepes (pH 7.4) containing 100 mM dithiothreitol (DTT). 2′,5′-ADP Sepharose 4B was purchased from Pharmacia-LKB Biotechnology Inc. DEAE Bio-Gel A, Coomassie Blue R-250, and Bradford protein dye reagent were purchased from Bio-Rad. Reaction vials were purchased from Pierce Chemical Co. Centrifugal filtration units (Ultrafree-15, Biomax-50K NMWL membrane) were purchased from Millipore. NHA was purchased from Alexis Corp., and citrulline contamination was determined to be less than 2% as analyzed by HPLC. Other reagents were purchased from Sigma.

Bacterial Expression Vector for iNOS. The pCWiNOS expression vector was constructed by assembling three fragments of the iNOS gene in pGEM-4Z and then subcloning the entire gene into pCW. An *Nde*I site was added at the ATG start site by polymerase chain reaction amplification with the 5′ primer CTAGCCCATATGGCTTGCCCCTGGAAGTT and the 3′ primer TGAAACATTTCCTGTGCTGTGCTAC. The PCR product was cut with *Nde*I/*Bam*HI. The middle fragment of the iNOS gene was cut from pBluescript II KS with *Bam*HI/*Acc*I. Stop codons, TAG and TAA, and a *Hin*dIII site were added after the natural stop codon by PCR amplification with the 5′ primer CTGTTCCAGGTGCACACAGGCTACTC and the 3′ primer GCGCGCAAGCTTACTATCAGAGCCTCGTGGCTTT. The PCR product was cut with *Acc*I/*Hin*dIII. The three iNOS fragments were assembled one at a time in pGEM-4Z using the appropriate restriction enzymes to make pGEMiNOS. The entire iNOS gene (from pGEMiNOS cut with *Nde*I/*Hin*dIII) was ligated into pCW to make pCWiNOS. Mutations and fidelity of the PCR reactions were confirmed by DNA sequencing. All primer synthesis and DNA sequencing were performed by the University of Michigan Biomedical Research Core Facility.

Expression of iNOS. Coexpression of iNOS and CaM was necessary for significant expression of soluble, active NOS. An overnight culture of JM109-pCWiNOS-pACYC:CaM2-1 was used to inoculate (1:100) larger cultures of Terrific Broth media (12 g/L tryptone, 24 g/L yeast extract, 4 mL/L glycerol, 17 mM KH_2PO_4, and 72 mM K_2HPO_4) containing 50 μg/mL ampicillin and 34 μg/mL chloramphenicol at 37 °C. At an A_{600} of ~0.5, the culture was cooled to 25 °C and induced by the addition of 1 mM IPTG (final concentration). After approximately 24 h of growth at 25 °C, the cells were pelleted at 5300*g*, transferred to 50 mL conical tubes, and stored at −80 °C.

Purification of iNOS. Cell pellets from 0.5−1.5 L of culture were resuspended in sonication buffer (50 mM Hepes, pH 7.4, 10% glycerol, 10 μg/mL benzamidine, 5 μg/mL leupeptin, and 1 μg/mL each of pepstatin, chymostatin, and antipain) and lysed by sonication. Centrifugation for 1 h at 100000*g* yielded supernatant which was stored at −80 °C. The purification of iNOS was modified from Hevel and Marletta (*7*). NOS in the 100000*g* supernatant (5−7 units; 1 unit is defined as that amount of NOS required to produce 1 μmol of •NO/min) was purified using 1 g of 2′,5′-ADP Sepharose 4B resin and 2 mL of DEAE Bio-Gel A resin with concentration in an Ultrafree-15 centrifugal ultrafiltration device. All buffers, except the 120 mM NaCl elution buffer for the DEAE resin, contained 5 mM arginine. Purified enzyme was subjected to three 1.5 mL washes of 100 mM Hepes, pH 7.4, in the ultrafiltration device. H_4B is not present in *E. coli* lysates (*24*), and, therefore, NOS is expressed without H_4B bound (*25*). The omission of H_4B from all buffers during purification and concentration steps resulted in NOS with no bound pterin (H_4B-free NOS). The inclusion of 10−20 μM H_4B (140−280 μM DTT) in all buffers during sonication, purification, and concentration steps resulted in NOS (holoNOS) exhibiting a 5−15% rate enhancement of •NO production with exogenously added H_4B as measured by the oxyhemoglobin assay (*26*). Protein concentration was determined by either the Bradford protein assay or the BCA protein assay (Pierce) using bovine serum albumin as a standard, or the absorbance of the substrate-bound holoNOS heme Soret band with an extinction coefficient of 100 000 M^{-1} cm^{-1} at 393 nm (*27*). NOS purified by this method was greater than 95% pure as judged by SDS−PAGE stained with Coomassie Blue R-250. Purified holoNOS was stored with 10−30 μM additional H_4B and 20% glycerol at −80 °C. Purified H_4B-free NOS was stable stored at concentrations greater than 20 μM with 50% glycerol at −80 °C.

Assays of NOS Reactions. (*A*) *•NO Detection.* The formation of •NO was detected by two methods: the oxidation of oxyhemoglobin and the reaction of •NO with ozone to form a chemiluminescent species. For the latter method, a Sievers Model 270 •NO chemiluminescence detector (Boulder, CO) connected to a Hewlett-Packard 3396A integrator was used. Aqueous samples from NOS reactions (50 μL) were injected directly into a glass manifold containing 5 mL of 1 M NaOH, 0.2% antifoam SO-25. Continuous flow of nitrogen through the manifold and

operation of a vacuum pump downstream of the detector resulted in •NO from the injected sample entering the detector. The detection limit of the instrument reported by the manufacturer is ~10 fmol of •NO.

(*B*) *Amino Acid Quantitation*. Reverse-phase HPLC of *o*-phthalaldehyde (*o*-PA) or 2,3-naphthalenedicarboxaldehyde (NDA) derivatives with absorbance detection was carried out as previously described (*19*), using an HP 1090 Series II instrument with a diode array detector. For *o*-PA derivatization, the injector was programmed to add 15 μL of 6 mM *o*-PA, 86 mM 2-mercaptoethanol, 1.0 M potassium borate, pH 10.4, to a vial containing 25 μL of sample or standard. The reaction solutions were then mixed by draw and eject cycles over 4 min, followed by injection of a 25 μL aliquot of the reaction mixture. *o*-PA derivatization conditions resulted in the quantitative conversion of CN-orn in the sample to citrulline. For NDA derivatization, 5 μL of 1 mM DTT was added to a vial containing 20 μL of sample or standard and the injector programmed to add 10 μL of 50 mM NaCN, 1.0 M potassium borate, pH 9.5, and 5 μL of 10 mM NDA in methanol. The reaction was mixed by several draw and eject cycles. After approximately 15 min, 25 μL of the reaction was injected. NDA derivatization conditions allow the separation and quantification of N^{δ}-cyanoornithine independently from citrulline. Citrulline and NHA standards were used to quantify the samples.

(*C*) *NO_2^-/NO_3^- Determination*. Nitrate reductase (34 milliunits; 5 μL of 7.6 mg/mL stock; 1 unit reduces 1.0 μmol of nitrate/min at pH 7.5, 25 °C; Sigma, from *Aspergillus*) and 38 μM NADPH (5 μL of 7 mM) were added to 80 μL of sample to reduce nitrate to nitrite. After approximately 1 h at room temperature, 100 milliunits of glutamate dehydrogenase (5 μL of 1:110 dilution of 2200 units/mL stock; 1 unit reduces 1 μmol of α-ketoglutarate to L-glutamate/min at pH 7.3, 25 °C, with the concomitant oxidation of NADPH; Sigma, type II, from bovine liver), 4 mM α-ketoglutarate, and 100 mM NH_4Cl (5 μL of 80 mM α-ketoglutarate, 2.0 M NH_4Cl) were added to each sample and allowed to sit at room temperature for 10−20 min in order to oxidize the remaining NADPH. Total sample NO_2^- and standards were then quantified by the Griess reaction as described in the Cayman Chemical Co. assay kit.

(*D*) *NOS Electron-Transfer Reactions*. Rates of NADPH oxidation were determined on a Beckman DU 640 spectrophotometer with a Peltier Temperature Controller by recording the decrease in absorbance at 340 nm over time (ϵ = 6200 M^{-1} cm^{-1}). Assays were carried out at 25 °C with 0 or 1 mM substrate (arginine or NHA), 2.5−34 μg of H_4B-free NOS, 100 mM Hepes, pH 7.4, and initiated by the addition of 120 μM NADPH in a total volume of 200 μL.

Cytochrome *c* reduction by NOS was followed as an increase in absorbance at 550 nm ($\Delta\epsilon$ = 21 000 M^{-1} cm^{-1}). Assays (500 μL) at 37 °C consisted of 50 μM cytochrome *c*, 1.25 μg H_4B-free NOS, 100 mM Hepes, pH 7.4, 0 or 1 mM arginine or NHA and were initiated with 120 μM NADPH.

(*E*) *Enzyme Reactions*. Assays were carried out at 25 °C. Reactions with NADPH contained 1 mM NHA or arginine, 300−500 μM NADPH, 50 μM phenylalanine (HPLC internal standard), and 100 mM Hepes, pH 7.4, and were initiated by the addition of 2.5−10 μg of H_4B-free NOS (25 μL total assay volume). These reactions were quenched at specified times by the addition of 15 μL of the previously described *o*-PA mixture. After 3−4 min derivatization time, 25 μL of the reaction was analyzed by HPLC. Phenylalanine included in the assay showed no effect on the enzyme reaction when compared to reactions where phenylalanine was added after quenching. For chemiluminescence analysis, 50 μL assays were used without quenching. Assays (50 μL) of CO inhibition were similarly composed. H_4B-free NOS and 100 mM Hepes, pH 7.4 (44 μL) in vented 1 mL reaction vials were equilibrated for 10−15 min at room temperature either under a constant flow of an 80:20 mixture of CO/O_2 or open to air. Reaction vials were then sealed and brought to 25 °C in a water bath. The reactions were initiated with the addition of NADPH and NHA (6 μL; for CO samples, stock solution was previously purged with the CO mixture in a reaction vial) with a gastight syringe, quenched by the addition of 30 μL of *o*-PA mixture after 4 min, and a 25 μL aliquot was assayed by HPLC. Reactions with hydrogen peroxide (H_2O_2) contained 1 mM NHA or arginine, 150 mM H_2O_2, 50 μM phenylalanine, and 100 mM Hepes, pH 7.4, and were initiated with 4−5 of μg H_4B-free NOS (24 μL total assay volume). These reactions were quenched at specified times by the addition of 40 units of catalase (1 μL of 1:20 dilution of 798 units/μL stock; 1 unit decomposes 1 μmol of H_2O_2/min at pH 7, 25 °C; Sigma, from bovine liver). Amino acid products were analyzed by HPLC as previously described. Duplicate end-point assays for stoichiometry determinations contained 7 μg of H_4B-free NOS, 1 mM NHA, 100 mM Hepes, pH 7.4, and 0, 5, 10, 15, 20, 25, or 30 μM NADPH in 25 μL. The reactions were incubated at room temperature for 30 min to 1 h and subsequently analyzed for amino acid product formation by HPLC.

(*F*) *K_M Determination of NHA*. Duplicate assays (25 μL final volume) included 100 mM Hepes, pH 7.4, 7.3 μg H_4B-free NOS, 0.02−2 mM NHA, 300 μM NADPH, and 50 μM phenylalanine. Additional assays contained 100 mM Hepes, pH 7.4, 2 μg of holoNOS, 7.5−1000 μM NHA, 300 μM NADPH, and 50 μM phenylalanine. All assays were initiated by the addition of NOS and were terminated after 4 min (H_4B-free NOS) or 1 min (holoNOS) at 25 °C with 15 μL of *o*-PA mixture. The products were analyzed by HPLC. Contaminating citrulline, determined from identical assays without NOS, was subtracted at each NHA concentration. This amount of citrulline was less than 2% that observed in the presence of NOS.

Spectral Studies. UV−Vis spectroscopy was carried out with a Cary 3E spectrophotometer equipped with a circulating water bath maintaining a temperature of 37 or 25 °C.

(*A*) *Reduction and CO Complex Formation of H_4B-Free NOS*. H_4B-free NOS in 100 mM Hepes, pH 7.4, with 0 or 1 mM NHA in an anaerobic cuvette was continuously flushed with carbon monoxide (CO, 99.999% pure, Matheson Gas Products, Inc.) for 10−15 min on ice. An aliquot of anaerobic NADPH (subjected to cyclical vacuum-line evacuation and purified argon flushing) or a few grains of solid sodium dithionite were added to the cuvette. Heme reduction was confirmed by formation of a reduced heme−CO complex absorbing at 445 nm.

(*B*) *Nitrosyl Complex Formation*. The ferrous form of the heme domain β1(1−385) of soluble guanylate cyclase (sGC) (*28*) was oxidized by the addition of 1.1 equiv of potassium ferricyanide. The sample was then passed over a PD10

desalting column (Pharmacia-LKB Biotechnology, Inc.) and kept at 4 °C. Ferric β1(1−385) (4.8 μM final heme concentration) was added to an aerobic solution of 0.1 or 0.3 μM H_4B-free NOS, 2 mM NHA, and 100 mM Hepes, pH 7.4. The spectral contribution of H_4B-free NOS was negligible in the region 450−650 nm. The cuvette was equilibrated to 25 °C over 2−3 min and the reaction initiated by the addition of 200 μM NADPH. Spectra (scanning from 800 to 300 nm) were recorded 30 s after initiation and every minute thereafter up to 20 min.

NOS nitrosyl complex formation during turnover was initiated by the addition of 100 μM NADPH to a cuvette containing 2.5 μM H_4B-free NOS and 2 mM NHA in 100 mM Hepes, pH 7.4. This experiment was carried out aerobically at 25 °C. Spectra were recorded as described above.

Gel Filtration. Samples (50 μL) of H_4B-free NOS immediately following purification and after 1−5 h at 25 °C (±20−50 μM H_4B, 280−690 μM DTT) were applied to a Tosohaas GFC 300 GL (15 cm, 5 μm) column equilibrated with 100 mM NaCl, 50 mM Hepes, pH 7.4, and the effluent was monitored at 280 nm. At a flow rate of 0.8−1.0 mL/min, purified NOS eluted in two bands, the absorbance maxima separated by 0.5 min. The faster eluting peak corresponded to dimeric NOS and the slower to monomeric NOS.

RESULTS

Characterization of Recombinant iNOS. The presence of H_4B during iNOS expression was not required for expression of active protein in *E. coli*. The coexpression of calmodulin, however, was required for expression of active, soluble enzyme as previously observed (*23*, *29*). The inclusion of H_4B in the sonication and purification buffers resulted in the isolation of holoNOS with a •NO-forming activity of 0.78−1.0 μmol min^{-1} mg^{-1} measured by the oxyhemoglobin assay at 37 °C with arginine as the substrate. The recombinant enzyme had identical spectral properties (ferric heme, reduced heme−CO complex) and similar affinity for arginine (spectral binding constant; K_D = 13.5 μM) as the enzyme isolated from murine macrophages. The heme content of the purified recombinant enzyme was determined to be approximately 0.7/monomer by a modified hemochromagen assay (*13*, *30*).

Initial Characterization of H_4B-Free NOS. As shown in Figure 1, the UV−Vis spectrum of purified H_4B-free NOS exhibits a ferric low-spin heme Soret band at 418−422 nm. Addition of ≥1 mM arginine or NHA resulted in only a partial shift of the spectrum to high-spin ferric heme, exhibiting a broad Soret band centered around 404 nm. The low- to high-spin conversion was fast (finished in the time required to mix the sample) and incomplete. Assays of H_4B-free NOS in the presence of 1 mM arginine or NHA did not result in an observable rate of oxyhemoglobin oxidation. When 10 μM H_4B was added to similar assays before initiation with H_4B-free NOS, •NO production was observed (by oxyhemoglobin oxidation) with either arginine or NHA as the substrate. The specific activity of several preparations assayed in this manner was 0.33−0.56 (arginine) and 0.61−0.85 (NHA) μmol •NO min^{-1} mg^{-1} at 37 °C. The addition

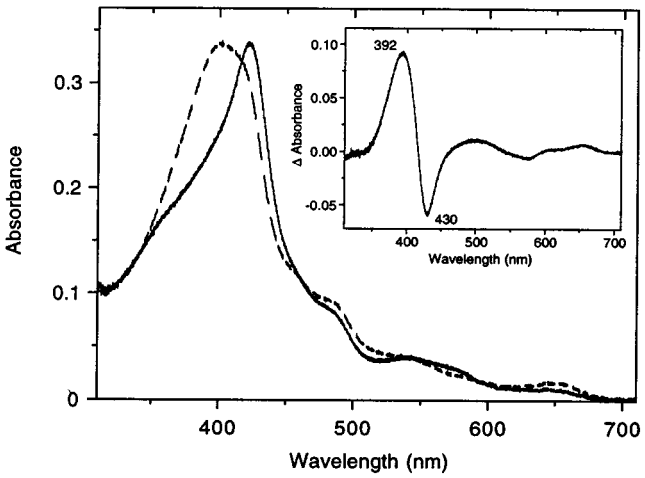

FIGURE 1: Spectra of holoNOS and H_4B-free NOS. The spectrum of holoNOS (dashed line) in the presence of 10 μM H_4B has a Soret peak at 400 nm. The absorbance maximum of H_4B-free NOS (solid line) is at 422 nm. The inset shows the calculated difference spectrum for H_4B bound to NOS, with an absorbance maximum at 392 nm and a minimum at 430 nm.

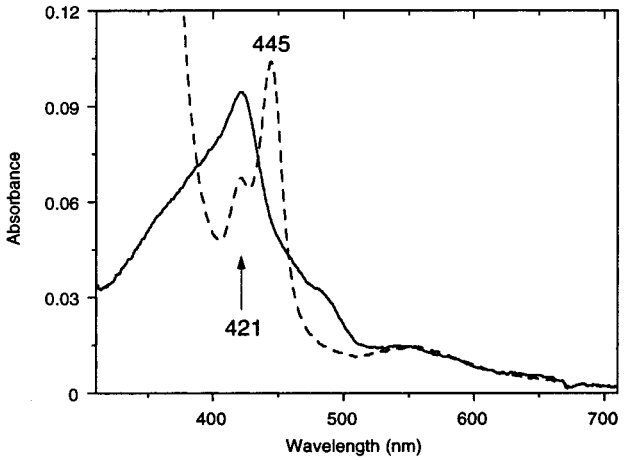

FIGURE 2: Reduction and CO complex formation of H_4B-free NOS. The spectrum of H_4B-free NOS (solid line) was recorded after equilibration of a quartz cuvette containing the enzyme with CO gas for 10 min. The enzyme was reduced with sodium dithionite and the spectrum of the reduced heme−CO complex (dashed line) subsequently recorded. The complex has absorbance maxima at 421 and 445 nm.

of exogenous Ca^{2+} and calmodulin to the assay had no effect on the activity. Reduction of the enzyme with dithionite or NADPH in the presence of CO resulted in the formation of a characteristic peak at 445 nm (Figure 2). Reduction of cytochrome *c* by H_4B-free NOS occurred at a rate of 22 ± 1 (n = 4) μmol min^{-1} mg^{-1} NOS in the presence or absence of arginine or NHA (Table 1), similar to the rate observed for holoNOS. At 37 °C, H_4B-free NOS oxidized NADPH at 0.087 ± 0.017 (n = 7; no substrate), 0.152 ± 0.015 (n = 6; +1 mM arginine), and 0.386 ± 0.035 (n = 7; +1 mM NHA) μmol min^{-1} mg^{-1}. Rates of NADPH oxidation by H_4B-free NOS at 25 °C were 0.040 ± 0.005 (n = 4) μmol min^{-1} mg^{-1} in the absence of substrate and 0.108 ± 0.011 (n = 5) μmol min^{-1} mg^{-1} in the presence of 1 mM NHA.

Gel Filtration of H_4B-Free NOS. H_4B-free NOS subjected to gel filtration immediately following purification (0.33−0.45 μmol min^{-1} mg^{-1} with H_4B and arginine in assay) chromatographed as a mixture of monomers and dimers

Table 1: Activities of iNOS

	μmol min^{-1} mg^{-1}		
	H_4B-free NOS	H_4B-reconstituted NOS	holoNOS
citrulline formation[b]			
H_2O_2	0.120 ± 0.014 ($n = 6$)	not determined	0.815 ± 0.030 ($n = 2$)
NADPH	0.031 ± 0.006 ($n = 7$)	not determined	0.171 ± 0.020 ($n = 4$)
NADPH oxidation[e]			
no substrate	0.040 ± 0.005 ($n = 4$)	not determined	not determined
1 mM NHA	0.108 ± 0.011 ($n = 5$)	not determined	not determined
•NO formation[c]			
from arginine	none detected[b]	0.9−1.2	0.78−1.0
from NHA	none detected[b]	1.4−2.0	1.5−2.0
cytochrome *c* reduction[d]	22 ± 1 ($n = 4$)	not determined	21−27[a]

[a] NOS isolated from macrophages (*33*, *34*). [b] Assays were carried out at 25 °C with 1 mM NHA as the substrate. [c] Oxyhemoglobin assays were carried out at 37 °C with 100 μM NADPH. [d] Assays were carried out at 37 °C. [e] Assays were carried out at 25 °C.

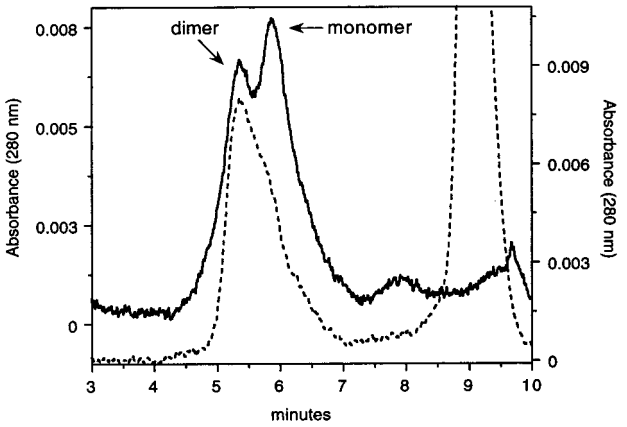

FIGURE 3: Gel filtration of H_4B-free and H_4B-reconstituted NOS. After 2 h at 25 °C, a dilute sample of H_4B-free NOS (solid line) was applied to a gel filtration column and the chromatogram recorded (left axis). The protein peak eluting at 5.3 min corresponds to dimeric NOS. The peak eluting at 5.8 min corresponds to monomeric NOS (determined by dissociation of NOS dimers in the absence of H_4B and the presence of DTT). A sample of NOS maintained at 25 °C for 2 h in the presence of 50 μM H_4B (690 μM DTT) was similarly analyzed (dashed line; right axis). NOS eluted in essentially one peak at 5.3 min. The absorbance at 9 min in this chromatogram was due to excess H_4B eluting after NOS.

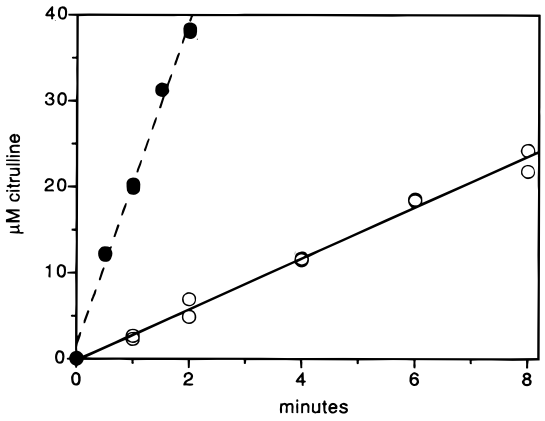

FIGURE 4: Time course of product formation from NHA at 25 °C. Amino acid products were derivatized with *o*-PA and analyzed by HPLC. Each time point was assayed in duplicate. The amount of citrulline found in the absence of either H_2O_2 or NADPH (usually <2% of NHA concentration) was subtracted from all points. Solid circles represent assays done with H_2O_2 as a substrate (dashed line), while open circles represent assays done with NADPH as a substrate (solid line).

(Figure 3). Aliquots analyzed at earlier times exhibited greater absorbance in the dimer peak than in the monomer. Over the course of several hours at 25 °C, the proportions of monomer absorbance increased at the expense of dimer absorbance (data not shown). This occurred in conjunction with up to an 80% decrease in the specific activity of the enzyme assayed with arginine and H_4B. When 50 μM H_4B was added to H_4B-free NOS and the sample chromatographed after 1−5 h at 25 °C, more than 90% of the absorbance eluted at the dimer retention time (Figure 3). Arginine had little to no effect on the H_4B-free NOS monomer:dimer equilibrium. When the samples that had been incubated with H_4B alone or with both arginine and H_4B were assayed by the oxyhemoglobin assay, a specific activity of 0.90−1.20 μmol min^{-1} mg^{-1} was measured.

Amino Acid Products of H_4B-Free NOS Reactions. H_4B-free NOS was not stable at 37 °C, and reactions other than NADPH oxidation carried out at that temperature did not show a linear time dependence under the experimental conditions described. However, at 25 °C, H_4B-free NOS was much more stable and exhibited linear reaction kinetics. Therefore, all kinetic parameters described below were obtained at 25 °C. HPLC analysis of H_4B-free NOS reactions with H_2O_2 revealed the production of citrulline and CN-orn from NHA, as previously observed with neuronal holoNOS (*19*). Product formation was linear up to 2 min at 25 °C (Figure 4; Table 1) and dependent upon the inclusion of H_2O_2, NHA, and H_4B-free NOS. As with holoNOS (*18*, *19*), no products were observed from assays with arginine and H_2O_2.

NADPH supported the H_4B-free NOS-catalyzed formation of citrulline and CN-orn from NHA at 25 °C (Figure 4; Table 1). In contrast, holoNOS-catalyzed reactions with NHA and NADPH produced exclusively citrulline as the amino acid product (*19*) (J. M. Spanbauer and M. A. Marletta, unpublished results). Additionally, H_4B-free NOS did not catalyze any product formation from arginine in the presence of NADPH. Formation of amino acid products required NADPH, NHA, and H_4B-free NOS and exhibited a dependence on time and enzyme concentration. At 25 °C, the $K_{M,app}$ for NHA in the H_4B-free NOS reaction was 129 ± 9 μM ($n = 2$) as compared to 36.9 ± 0.3 μM ($n = 2$) in the holoNOS reaction. Equivalent assays of holoNOS at 25 °C containing 20 μM exogenous H_4B were 6.8-fold faster than that catalyzed by H_4B-free NOS for the H_2O_2 reaction and 5.5-fold faster for the NADPH/O_2 reaction (Table 1). The NADPH-dependent oxidation of NHA in the presence and

absence of H_4B results in different products. This altered chemistry may be responsible for the slower rate in the absence of H_4B. In addition, the absence of H_4B appears to decrease the rate of heme reduction by NADPH in the presence of CO (K.M.R. and M.A.M., unpublished results). It is unclear whether this is a direct effect of H_4B binding (i.e., due to heme spin state change) or an indirect effect (i.e., pertubation of protein tertiary structure to facilitate electron-transfer pathways). In the absence of H_4B, slowed heme reduction could become rate-limiting, thereby resulting in slower turnover.

Inorganic Product Identification. The inorganic product of the reaction of H_4B-free NOS, NHA, and NADPH was analyzed by several methods. Direct measurement of •NO by chemiluminescence detection ruled out the production of •NO in the reaction. The lack of detection is not due to insufficient production of •NO as identical reaction conditions produce more than sufficient quantities of citrulline as analyzed by HPLC. Chemiluminescent analysis of H_4B-reconstituted NOS reactions with NHA and NADPH identified significant amounts of •NO. As •NO formation is not detected in the H_4B-free NOS reaction, an alternative candidate for the inorganic product of the reaction is the nitroxyl anion (NO^-). NO^- produced by the reaction of holoNOS, NHA, and H_2O_2 has been observed to yield NO_2^-/NO_3^- as aerobic decomposition products (*18*). NO_2^-/NO_3^- were subsequently identified as stable products of the H_4B-free NOS reaction. Formation of NO_2^-/NO_3^- was determined to be essentially equimolar with amino acid product formation (NO_x^-/citrulline $= 0.94 \pm 0.10$; $n = 9$). These data suggest that under these reaction conditions (slow catalytic rate, presence of ferric heme of NOS, aerobic solution) protonation of NO^- with subsequent dimerization and dehydration to form N_2O does not occur to a significant extent.

Additional characterization of the initial inorganic product was accomplished by electronic absorption spectroscopy through the formation of heme−nitrosyl complexes. Ferric and ferrous heme−nitrosyl complexes of heme proteins, in particular those of iNOS (*31*) and β1(1−385), the heme domain of soluble guanylate cyclase (*28*), have previously been characterized. Ferrous β1(1−385) reacts with •NO to form a ferrous heme−nitrosyl complex with absorbance maxima at 399, 537, and 572 nm. Ferric β1(1−385) should bind NO^- to form a stable ferrous nitrosyl. The H_4B-free NOS reaction with NHA and NADPH was carried out in the presence of ferric β1(1−385). Only ~8% (0.4 μM) of the protein formed a ferrous nitrosyl complex (data not shown). The complex had an absorbance maximum at 574 nm in the difference spectrum which can be compared to the reported absorbance maximum at 572 nm in the absolute spectrum of the ferrous nitrosyl complex (*28*).

Formation of ferrous and ferric nitrosyl complexes of NOS during turnover has been observed with arginine and NADPH (*31*, *32*) as well as with NHA and H_2O_2 (*18*). Addition of NADPH to a cuvette containing ferric H_4B-free NOS and NHA resulted in the formation of a small amount (approximately 5%) of a transient spectral intermediate (Figure 5). In the first few minutes of the reaction the intermediate was characterized by absorbance maxima in the difference spectra at 442 and 577 nm. At later times, oxidation of the flavins and heme obscured the spectrum. The absorbance maxima of the intermediate suggest that it is predominantly a ferrous nitrosyl complex.

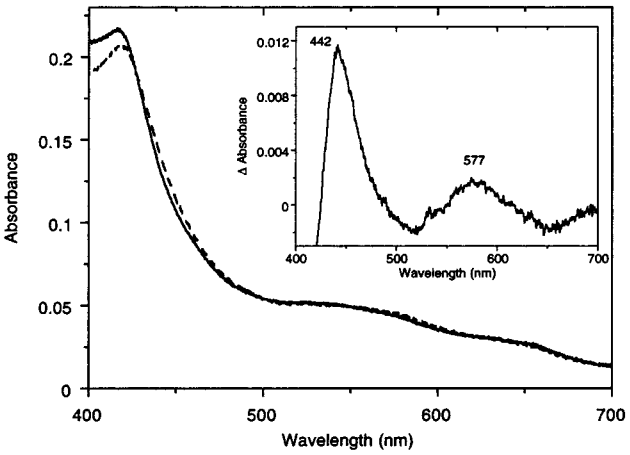

FIGURE 5: Spectrum of a transient complex formation from H_4B-free NOS, NHA, and NADPH under aerobic conditions at 25 °C. The initial spectrum (solid line) was recorded 30 s after initiation of the reaction and shows the Soret band at 418 nm. A spectrum of the reaction recorded after 4 min is also shown (dashed line). The Soret absorbance at 418 nm has decreased, and there is an increase in absorbance in the regions 435−490 and 560−600 nm. The inset shows the calculated difference spectrum for the transient intermediate formed during turnover, with absorbance maxima at 442 and 577 nm.

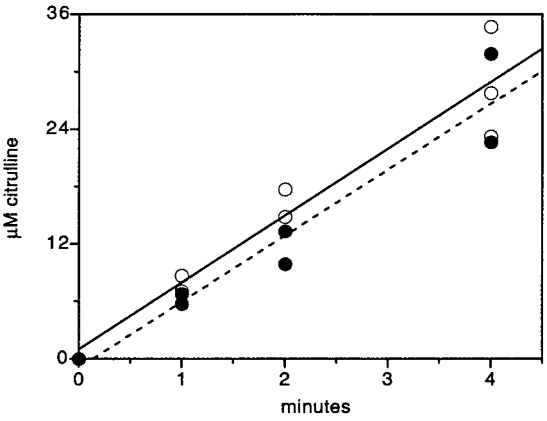

FIGURE 6: Effect of catalase on product formation from NHA at 25 °C. Assays were performed as described in Figure 4 and under Experimental Procedures. Assays in the absence of catalase (solid line) are represented by open circles. Assays in the presence of 50 units of catalase (dashed line) are represented by solid circles. The data are not significantly different within the error of the experiment.

Effects of Catalase and CO. Assays of H_4B-free NOS with NHA and NADPH were performed in the presence and absence of 50 units of catalase. In two separate experiments, no significant difference in the rate of citrulline formation in the presence or absence of catalase was observed (Figure 6). H_4B-free NOS assays were also equilibrated with either an 80:20 mixture of CO/oxygen or ambient air and initiated with NHA and NADPH. CO inhibited the reaction approximately 69% (Table 2).

DISCUSSION

We have approached the question of the function of NOS-bound H_4B by examining the properties of the enzyme in the absence of H_4B. NOS isolated with substoichiometric H_4B bound exhibits a variable ratio of low- to high-spin heme

Table 2: Effect of CO on Amino Acid Product Formation from NHA by H_4B-Free NOS at 25 °C

	nmol of citrulline min^{-1} mg^{-1}		% inhibition
	air	80:20 ($CO:O_2$)	
experiment #1	34.7 ± 1.1 ($n = 2$)	11.0 ($n = 1$)	68
experiment #2	27.4 ± 6.3 ($n = 3$)	8.6 ± 0.3 ($n = 3$)	69

as assessed by electronic absorption spectroscopy (*25*) (J. M. Hevel and M. A. Marletta, unpublished results). Consistent with these observations, iNOS purified from *E. coli* in the absence of H_4B is predominantly[2] low-spin (420 nm absorbance maximum). Addition of substrates (arginine or NHA) did not shift the heme Soret band completely to 395 nm. H_4B has a distinct influence on the low- to high-spin heme equilibrium and is required, in addition to substrate, for the complete formation of high-spin NOS. Also, H_4B has previously been observed to affect the oligomeric state of the enzyme (*33*−*35*). Specifically, H_4B promotes and stabilizes the dimeric form of NOS. We have obtained similar results, although essentially complete reconstitution of NOS dimer required only the presence of H_4B and at least a 1 h incubation. Samples of H_4B-free NOS treated in this manner also exhibited a maximal specific activity that was comparable to holoNOS specific activity. Therefore, full reconstitution of the •NO-forming activity and, presumably, H_4B binding to H_4B-free NOS were accomplished. The large amount of P445 formed relative to P420 upon the reduction of NOS with either NADPH or dithionite in the presence of CO is additional evidence for the native environment of the heme in this form of the enzyme. These results demonstrate the viability of the H_4B-free NOS used in these studies and the absence of any irreversible damage done to the enzyme.

Identification of the inorganic product of the H_4B-free NOS-catalyzed reaction with NHA and NADPH was approached by several different methods. Chemiluminescent analysis of reactions eliminated •NO as the identity of the inorganic product. However, the stable end products detected in the reaction were NO_2^- and NO_3^-. NO^- had already been identified as a product of the H_2O_2-supported reaction of holoNOS and NHA (*18*) and was a strong candidate for the product of the NADPH-supported H_4B-free NOS reaction. The ferric form of the heme domain of sGC [β1(1−385)] was utilized to trap NO^- and form a stable ferrous nitrosyl−heme complex, but only a small percentage of the complex was formed. The poor binding of NO^- may be analogous to the weak binding of anions by the ferric heme of sGC (heterodimer of α1 and β1 subunits), observed previously with cyanide (*36*). For cyanide binding to sGC, the k_{on} and k_{off} were determined to be $(7.8 \pm 0.3) \times 10^{-2}$ M^{-1} s^{-1} and $(7.2 \pm 0.2) \times 10^{-5}$ s^{-1}, respectively. Therefore, millimolar concentrations of NO^- might be required to bind a significant amount of ferric sGC. Achievement of high concentrations of NO^- formed by H_4B-free NOS is hampered both by the slow catalytic rate of H_4B-free NOS and by the rapid decomposition of NO^- in aerobic solutions.

The observation that NOS nitrosyl complexes could be formed during turnover (*18*, *31*, *32*) led us to attempt a similar experiment with H_4B-free NOS. A small amount of a spectral intermediate entirely consistent with an NOS ferrous nitrosyl complex was formed. The ferrous nitrosyl complex of NOS exhibits a Soret band at 440 nm and a single broad α/β peak at 577 nm by difference spectroscopy (*31*). The spectral intermediate formed in this study had a sharp absorbance peak at 442 nm and a single broad absorbance peak at 577 nm in the difference spectrum (Figure 5, inset). This spectral intermediate formed within the first few minutes of the reaction. As the reaction progressed and NADPH was depleted, the NOS spectrum reverted to a mixed-spin ferric heme Soret band. These results are consistent with the formation of NO^- and the subsequent reaction with ferric NOS. The steady-state concentration of this complex is limited by instability in an aerobic environment, resulting in only a small percentage of complex formed. Thus, the inorganic product appears to be NO^-, which agrees with the results of the spectroscopy experiments and the aerobic decomposition to NO_2^-/NO_3^- as well as the lack of •NO detection in assays.

Identical products were determined here for the H_4B-free NOS reaction with NHA and NADPH and the previously reported holoNOS reaction with NHA and H_2O_2 (*18*, *19*). Therefore, confirmation that the H_4B-free NOS reaction was not H_2O_2-dependent was required. H_4B-free NOS oxidized NADPH at 94 nmol min^{-1} mg^{-1} in the presence of NHA (uncorrected for the 43 nmol min^{-1} mg^{-1} rate of oxidation in the absence of substrate), yet under identical conditions formed the products citrulline and CN-orn at only 30 ± 3 nmol min^{-1} mg^{-1}. This yields a stoichiometry of 3:1 (moles of NADPH oxidized:moles of product) when not corrected for uncoupled NADPH oxidation. End-point assays with limiting NADPH resulted in stoichiometries of (1.2−1.6):1. The current mechanistic proposal for •NO formation from NHA requires a half mole of NADPH oxidized per mole of product formed. With the formation of NO^- from NHA, we would expect to observe 1 mol of NADPH oxidized per mole of product formed. Therefore, H_4B-free NOS appears to be partially uncoupled with respect to NADPH oxidation, producing reduced oxygen species, perhaps including H_2O_2•. H_2O_2-dependent H_4B-free NOS catalysis in the presence of saturating NADPH and NHA is highly unlikely, however, since the $K_{M,app}$ for H_2O_2 is 30 mM (*18*). The H_4B-free NOS assays contained only 300−500 μM NADPH, allowing for maximally 300−500 μM H_2O_2 production if H_2O_2 was the sole and instantaneous product. Furthermore, addition of 50 units of catalase did not affect the rate of citrulline formation. This amount of catalase should be sufficient to decompose any H_2O_2 formed by NOS and released into solution. There still remains, however, the possibility that H_2O_2 formed in or near the enzyme active site, presumably by the flavins, was not released into solution and catalyzed the reaction by binding to the ferric heme.

CO was used in this study to assess whether heme reduction played an important role in the NADPH/O_2 reaction catalyzed by H_4B-free NOS. CO has previously been shown to inhibit the NADPH-catalyzed oxidation of both arginine and NHA by holoNOS (*13*, *17*). The formation of citrulline was inhibited approximately 57% with arginine and 33% with NHA as the substrate in the presence of an 80:20 mixture of CO/O_2. CO competes with oxygen as a ligand for the reduced heme. Neither the peroxide-supported

[2] High concentrations of glycerol (50% v/v) result in some high-spin enzyme. Upon dilution, the high-spin NOS converts to low-spin in minutes.

reactions of cytochrome P450 (*37*) nor the H_2O_2 reaction of holoNOS (*18*) is inhibited by CO since ferrous heme is not formed in these reactions. Inhibition of 69% (Table 2) of the H_4B-free NOS reaction with NHA and NADPH/O_2 compared to the reaction measured under air was observed. CO inhibition of the reaction is strong evidence for the direct involvement of a reduced heme in catalysis. Therefore, H_2O_2 formation from the flavins via uncoupled NADPH oxidation is not likely responsible for the chemistry observed with the substrates NADPH and NHA. Such H_2O_2-dependent catalysis would be inhibited by catalase, but, more importantly, does not require formation of ferrous heme.

Proposals for the NOS reaction mechanism have focused primarily on heme catalysis in the initial hydroxylation of arginine to NHA as well as the further oxidation of NHA to citrulline. The function of H_4B in the NOS reaction has been difficult to unravel. Although speculation on the usual function of H_4B as a cosubstrate in hydroxylation reactions has been advanced, little evidence for a catalytic H_4B role in the NOS reaction has emerged. We examined the reactions catalyzed by NOS in the absence of H_4B in order to investigate the role of this cofactor. Initially, H_4B-free NOS appeared to be inactive as no •NO was detected with NADPH and either arginine or NHA as substrates. However, HPLC analysis of the reactions with NHA did show the conversion of NHA to amino acid products. Both citrulline and CN-orn were identified as products of both the NADPH- and H_2O_2-supported reactions. HoloNOS, however, catalyzes the formation of citrulline as the sole amino acid product of the NADPH/O_2 reaction.

The mechanistic implications of these results are significant. First, H_4B-free NOS did not catalyze any reaction with arginine as a substrate, although products could be formed from NHA and NADPH. This lack of arginine reactivity in the absence of H_4B points to complete dependence of the first step of the NOS reaction on the presence of H_4B. This evidence, along with the absence of H_2O_2-supported chemistry with arginine, strongly implicates the involvement of H_4B in the *N*-hydroxylation of arginine to NHA. This step may, therefore, be envisioned as a classical pterin-dependent hydroxylation of arginine to NHA. By analogy to the pterin-dependent hydroxylases, we would also expect this reaction to require a non-heme metal ion functioning with the pterin in the first step of the reaction. In fact, the presence of stoichiometric non-heme iron bound to NOS has been recently discovered in our lab (*42*). The recent crystal structure of the iNOS heme domain dimer, however, shows the H_4B cofactor in a position relative to the bound substrate, arginine, that is not conducive for direct catalysis (*22*). However, this structure does not contain a non-heme iron and was only 0.55 occupied with arginine. The absence of this potential metal cofactor may very well affect the orientation of the substrate in the active site, leaving the potential for an alternate conformation. Also, in contrast to the previously characterized pterin-dependent hydroxylases, NOS apparently does not release dihydrobiopterin after each turnover (*16*, *38*). The implication is that NOS exhibits a unique reaction in which the reduced biopterin is regenerated with each catalytic cycle.

Second, the formation of NO^- instead of •NO in the NADPH-supported reaction suggests that H_4B is also involved in the oxidation of NHA. A three-electron oxidation

Scheme 1: Proposed Mechanisms of H4B-Dependent, One- and Two-Electron Oxidation of NHA

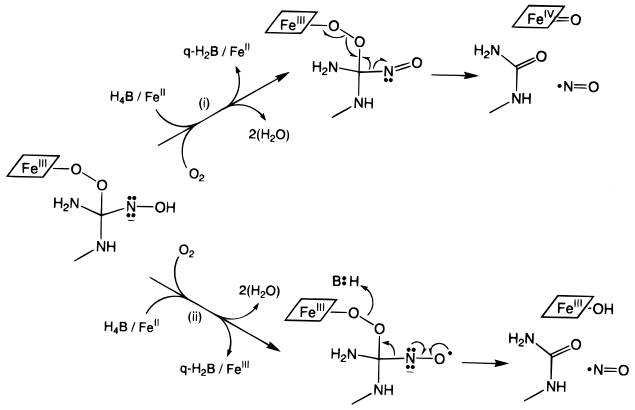

of NHA must occur to generate •NO. This can occur through a combination of one- and two-electron oxidations by heme and H_4B. We have previously proposed (*1*, *18*) that this step involves a one-electron oxidation of NHA by a ferrous dioxygen−heme complex. The results presented here, though, implicate H_4B in the oxidation of NHA. We will discuss four mechanisms by which NHA may be oxidized: (1) a H_4B-dependent, two-electron oxidation; (2) a H_4B-dependent one-electron oxidation; (3) a one-electron oxidation by a ferrous oxy−heme complex; (4) or a change in heme-derived oxidant.

In the first possibility (1), H_4B, in combination with a non-heme metal and O_2, could carry out a two-electron oxidation of NHA to generate a nitrosoamidine (Scheme 1, i). Before this oxidative step, an iron peroxide nucleophile (*18*, *39*, *40*) would form a tetrahedral intermediate with the substrate. Homolytic O−O bond scission and collapse of the tetrahedral intermediate would then generate the observed products, citrulline and •NO. In the absence of H_4B, H_4B-dependent NHA oxidation could not occur, and heterolytic O−O bond scission of the tetrahedral intermediate is required to result in the product NO^-. We would not be able to distinguish between a direct two-electron oxidation and a hydroxylation/dehydration step in this mechanism, because both would lead to equivalent products. In this mechanism, H_4B plays a direct role in the formation of products from NHA.

A H_4B-dependent one electron oxidation (2), on the other hand, could be envisioned as occurring via a high-valent, non-heme iron−oxo species formed from the reaction of a H_4B, O_2, and Fe^{2+} system (Scheme 1, ii). In this case, heterolytic O−O bond scission could occur to generate •NO. In the absence of H_4B, the reaction would simply proceed without the initial one-electron oxidation of NHA, yielding NO^-. In both mechanisms (1 and 2), three reducing equiv instead of two would be required to regenerate the H_4B/Fe^{2+}/ferric heme system.

These two mechanisms require the reduction of two molecules of molecular oxygen with five electrons exogenously derived. If those reducing equivalents came solely from NADPH, the reaction with NHA would require 2.5 equiv of NADPH. The NADPH to •NO stoichiometry for the overall reaction with arginine as the substrate has been reported to be 1.5, while only 0.5 equiv of NADPH has been reported starting with NHA (*2*). However, these stoichiom-

Scheme 2: Proposed Mechanisms of Heme-Dependent NHA Oxidation

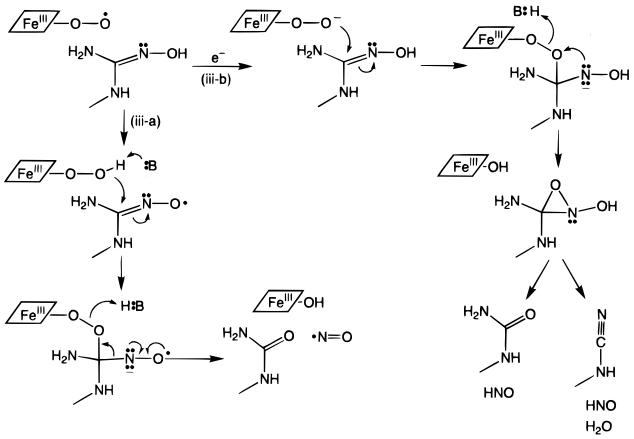

etries have been derived by subtracting the rate of NADPH oxidation in the absence of substrate from that observed in the presence of substrate. This would result in underestimation of the reducing equivalents required if NADPH oxidation was more coupled to product formation. The different NADPH stoichiometry may point toward a mechanism involving an alternative source of reducing equivalents.

Alternatively, the ferrous dioxygen−heme complex 3 could carry out the one-electron oxidation of NHA as previously proposed, form a tetrahedral intermediate with the substrate, undergo homolytic O−O bond scission, and collapse to the products citrulline and •NO (Scheme 2). The presence of H_4B could modulate the mechanism of reduction of the ferrous dioxygen complex. In the presence of H_4B, the ferrous dioxygen complex is reduced by NHA (Scheme 2, iii-a). In the absence of H_4B, the ferrous dioxygen complex is reduced by NADPH via the flavins (Scheme 2, iii-b). The origin of that reducing equivalent determines whether the inorganic product is •NO or NO^-. H_4B may cause this effect in several ways. H_4B binding affects the spin equilibrium of the heme. A change in the heme spin state has been correlated in other P450s with a change in the heme reduction potential. Alternatively, H_4B has been shown to accelerate the decay of the ferrous dioxygen complex of neuronal NOS (*41*). Transfer of the second reducing equivalent from either the substrate or the reductase domain may be influenced by the lifetime of the ferrous dioxygen complex. This mechanism implies an indirect, but significant, role for H_4B in the NHA reaction.

In addition, we cannot conclusively eliminate the possibility of a change in the heme-derived oxidant (4) in the absence of H_4B. Clague et al. have discussed the possibility of a change in the mechanism of the H_2O_2-supported reaction to involve a high-valent iron−oxo complex (*19*). The formation of citrulline and CN-orn in the H_4B-free NOS reaction may point to a similar change in mechanism. If the nucleophilic addition of the proposed iron-peroxo to NHA occurs in the absence of H_4B, however, and cyclization via the hydroxy-bearing nitrogen to generate an oxaziridine intermediate follows, both citrulline and CN-orn may be generated from a common intermediate as proposed by Clague et al. (Scheme 2, iii-b).

In summary, H_4B-free NOS can catalyze the formation of citrulline, CN-orn, and NO^- from NHA and either NADPH or H_2O_2. The products of the NADPH-supported reaction imply a role for H_4B in the NHA reaction. Whether this involves a direct role in oxidizing the substrate or an indirect role in modulating the reductive pathway of the ferrous oxy−heme complex is unclear. Of particular interest is the lack of arginine reactivity with H_4B-free NOS, particularly in light of the catalytic competence with NHA. The total dependence of the reaction of arginine on the presence of H_4B implies a direct catalytic role for H_4B.

ACKNOWLEDGMENT

We thank Yunde Zhao for his generous gift of the heme domain of sGC. We thank Amy R. Hurshman for her assistance in the development of the *E. coli* expression system and Melissa J. Clague for insightful mechanistic discussions. We also thank the members of the Marletta lab for helpful suggestions during the preparation of this paper.

REFERENCES

1. Marletta, M. A. (1993) *J. Biol. Chem. 268*, 12231−12234.
2. Stuehr, D. J., Kwon, N. S., Nathan, C. F., Griffith, O. W., Feldman, P. L., and Wiseman, J. (1991) *J. Biol. Chem. 266*, 6259−6263.
3. Pufahl, R. A., Nanjappan, P. G., Woodard, R. W., and Marletta, M. A. (1992) *Biochemistry 31*, 6822−6828.
4. Pollock, J. S., Förstermann, U., Mitchell, J. A., Warner, T. D., Schmidt, H. H. H. W., Nakane, M., and Murad, F. (1991) *Proc. Natl. Acad. Sci. U.S.A. 88*, 10480−10484.
5. Bredt, D. S., and Snyder, S. H. (1990) *Proc. Natl. Acad. Sci. U.S.A. 87*, 682−685.
6. Schmidt, H. H. H. W., and Murad, F. (1991) *Biochem. Biophys. Res. Commun. 181*, 1372−1377.
7. Hevel, J. M., White, K. A., and Marletta, M. A. (1991) *J. Biol. Chem. 266*, 22789−22791.
8. Stuehr, D. J., Cho, H. J., Kwon, N. S., Weise, M. F., and Nathan, C. F. (1991) *Proc. Natl. Acad. Sci. U.S.A. 88*, 7773−7777.
9. Nathan, C. (1992) *FASEB J. 6*, 3051−3064.
10. Stevens-Truss, R., and Marletta, M. A. (1995) *Biochemistry 34*, 15638−15645.
11. Mayer, B., John, M., Heinzel, B., Werner, E. R., Wachter, H., Schultz, G., and Böhme, E. (1991) *FEBS Lett. 288*, 187−191.
12. Richards, M. K., Clague, M. J., and Marletta, M. A. (1996) *Biochemistry 35*, 7772−7780.
13. White, K. A., and Marletta, M. A. (1992) *Biochemistry 31*, 6627−6631.
14. Stuehr, D. J., and Ikeda-Saito, M. (1992) *J. Biol. Chem. 267*, 20547−20550.
15. McMillan, K., Bredt, D. S., Hirsch, D. J., Snyder, S. H., Clark, J. E., and Masters, B. S. S. (1992) *Proc. Natl. Acad. Sci. U.S.A. 89*, 11141−11145.
16. Hevel, J. M., and Marletta, M. A. (1992) *Biochemistry 31*, 7160−7165.
17. Pufahl, R. A., and Marletta, M. A. (1993) *Biochem. Biophys. Res. Commun. 193*, 963−970.
18. Pufahl, R. A., Wishnok, J. S., and Marletta, M. A. (1995) *Biochemistry 34*, 1930−1941.
19. Clague, M. J., Wishnok, J. S., and Marletta, M. A. (1997) *Biochemistry 36*, 14465−14473.
20. Dix, T. A., and Benkovic, S. J. (1988) *Acc. Chem. Res. 21*, 101−107.
21. Kaufman, S. (1993) *Adv. Enzymol. 67*, 77.
22. Crane, B. R., Arvai, A. S., Ghosh, D. K., Wu, C., Getzoff, E. D., Stuehr, D. J., and Tainer, J. A. (1998) *Science 279*, 2121−2126.
23. Fossetta, J. D., Niu, X. D., Lunn, C. A., Zavodny, P. J., Narula, S. K., and Lundell, D. (1996) *FEBS Lett. 379*, 135−138.
24. Thöny, B., Leimbacher, W., Burgisser, D., and Heizmann, C. W. (1992) *Biochem. Biophys. Res. Commun. 189*, 1437−1443.

25. Rodriguez-Crespo, I., Gerber, N. C., and Ortiz de Montellano, P. R. (1996) *J. Biol. Chem. 271*, 11462−11467.
26. Hevel, J. M., and Marletta, M. A. (1994) *Methods Enzymol. 233*, 250−258.
27. Sono, M., Stuehr, D. J., Ikeda-Saito, M., and Dawson, J. H. (1995) *J. Biol. Chem. 270*, 19943−19948.
28. Zhao, Y., and Marletta, M. A. (1997) *Biochemistry 36*, 15959−15964.
29. Gerber, N. C., Nishida, C. R., and Ortiz de Montellano, P. R. (1997) *Arch. Biochem. Biophys. 343*, 249−253.
30. Fuhrhop, J. H., and Smith, K. M. (1975) in *Porphyrins and Metalloporphyrins* (Smith, K. M., Ed.) p 804, Elsevier Scientific Publishing Co., Amsterdam.
31. Hurshman, A. R., and Marletta, M. A. (1995) *Biochemistry 34*, 5627−5634.
32. Wang, J., Rousseau, D. L., Abu-Soud, H. M., and Stuehr, D. J. (1994) *Proc. Natl. Acad. Sci. U.S.A. 91*, 10512−10516.
33. Baek, K. J., Thiel, B. A., Lucas, S., and Stuehr, D. J. (1993) *J. Biol. Chem. 268*, 21120−21129.
34. Abu-Soud, H. M., Loftus, M., and Stuehr, D. J. (1995) *Biochemistry 34*, 11167−11175.
35. Klatt, P., Schmidt, K., Lehner, D., Glatter, O., Bächinger, H. P., and Mayer, B. (1995) *EMBO J. 14*, 3687−3695.
36. Stone, J. R., Sands, R. H., Dunham, W. R., and Marletta, M. A. (1996) *Biochemistry 35*, 3258−3262.
37. Nordblom, G. D., White, R. E., and Coon, M. J. (1976) *Arch. Biochem. Biophys. 175*, 524−533.
38. Giovanelli, J., Campos, K. L., and Kaufman, S. (1991) *Proc. Natl. Acad. Sci. U.S.A. 88*, 7091−7095.
39. Akhtar, M., Njar, V. C. O., and Wright, J. N. (1993) *J. Steroid Biochem. Mol. Biol. 44*, 375−387.
40. Akhtar, M., Corina, D., Miller, S., Shyadehi, A. Z., and Wright, J. N. (1994) *Biochemistry 33*, 4410−4418.
41. Abu-Soud, H. M., Gachhui, R., Raushel, F. M., and Stuehr, D. J. (1997) *J. Biol. Chem. 272*, 17349−17353.
42. Perry, J. M., and Marletta, M. A. (1998) *Proc. Natl. Acad. Sci. U.S.A. 95*, 11101−11106.

BI9813936